DOE/MC/25167-2986
(DE91002066)
Distribution Category UC-110

DOE/MC/25167--2986

DE91 002066

Solid Oxide Fuel Cell Processing Using Plasma Arc Spray Deposition Techniques

Final Report

E.R. Ray
C.J. Spengler
H. Herman

Work Performed Under Contract No.: DE-AC21-88MC25167

For
U.S. Department of Energy
Office of Fossil Energy
Morgantown Energy Technology Center
P.O. Box 880
Morgantown, West Virginia 26507-0880

By
Westinghouse Electric Corporation
Advanced Energy Conversion Department
Westinghouse Science and Technology Center
1310 Beulah Road
Pittsburgh, Pennsylvania 15235

July 1991

Table of Contents

Summary

The Westinghouse Electric Corporation, in conjunction with the Thermal Spray Laboratory of the State University of New York, Stony Brook, investigated the fabrication of a gas-tight interconnect layer on a tubular solid oxide fuel cell with plasma arc spray deposition. The principal objective was to determine the process variables for the plasma spray deposition of an interconnect with adequate electrical conductivity and other desired properties.

Plasma arc spray deposition is a process where the coating material in powder form is heated to or above its melting temperature, while being accelerated by a carrier gas stream through a high power electric arc. The molten powder particles are directed at the substrate, and on impact, form a coating consisting of many layers of overlapping, thin, lenticular particles or splats. The variables investigated were gun power, spray distance, powder feed rate, plasma gas flow rates, number of gun passes, powder size distribution, injection angle of powder into the plasma plume, vacuum or atmospheric plasma spraying, and substrate heating.

Typically, coatings produced by both systems showed bands of lanthanum rich material and cracking within the coating. Vacuum plasma sprayed coatings showed greater chemical inhomogeneity than atmospheric plasma sprayed coatings made with comparable spray parameters. Preheating the substrate reduced but did not eliminate internal coating cracking. A uniformly thick, dense, adherent interconnect of the desired chemistry was finally achieved with sufficient gas-tightness to allow fabrication of cells and samples for measurement of physical and electrical properties. A cell was tested successfully at 1000°C for over 1,000 hours demonstrating the mechanical, electrical, and chemical stability of a plasma-arc sprayed interconnect layer.

1. Introduction

The Westinghouse Electric Corporation and the State University of New York at Stony Brook undertook a 24-month research program to evaluate the feasibility and technical requirements of developing a solid oxide fuel cell that uses a plasma arc spray deposited interconnect strip. The plasma spray deposit concept is being considered for increased cell performance and reduced manufacturing cost.

The principal objective of the program was to determine the process variables for the fabrication of an interconnect strip deposited by plasma arc spray of oxide powder. In particular, the objectives were:

1. To form a gas impervious layer that resists degradation for 40,000 hours of service operation as a result of superior dopant chemistry and matched thermal expansion to the air electrode.

2. To deposit a layer of a particular chemistry for adequate electronic conductivity facilitating cell-to-cell interconnections.

3. To produce cells with a plasma arc sprayed interconnect strip which met a basic performance acceptance criterion.

All the plasma spray investigations in this program were conducted on porous zirconia tube-supported air electrodes. Details on the structure of the tubes are contained in Section 2 - Background.

2. Background

The current Westinghouse tubular solid oxide fuel cell (SOFC) design, shown in Figure 2.1, features a porous, calcia-stabilized zirconia support tube (12 to 13 mm OD), overlaid with a porous air electrode of modified lanthanum manganite (1.0 to 1.4 mm thick). A gas-tight electrolyte of yttria-stabilized zirconia, nearly 50 μm thick, covers the entire air electrode except for an area about 9 mm wide along the active cell length. This strip of exposed air electrode is covered by a thin (~30 μm), dense layer of magnesium-doped lanthanum chromite which serves as the electrical contacting area to the adjacent cell and is called the cell interconnection. The fuel electrode, a nickel-zirconia cermet, is about 150 μm thick and covers the entire electrolyte surface except in the vicinity of the interconnect region. The cell materials selected operate at high temperature (1000°C) and have thermal expansion coefficients which are closely matched to that of the porous support tube.

The variety of thermal-spray techniques, the diversity of processes for sprayable oxides, along with technologically advanced spray-control systems, afford an opportunity for commercial application of thermal spray technique to solid oxide fuel cells. Thermal spray technology has entered a new phase of industry acceptance as a viable process for "front end" manufacture rather than for repair and refurbishing. There are basically three types of thermal spray processes: plasma, combustion-flame, and two-wire electric arc that are available in state of the art commercial units. Plasma-arc spraying uses a thermal plasma (the highest temperature heat source and most suitable for making dense ceramic materials), and is the most technologically versatile thermal spraying process. Off-the-shelf

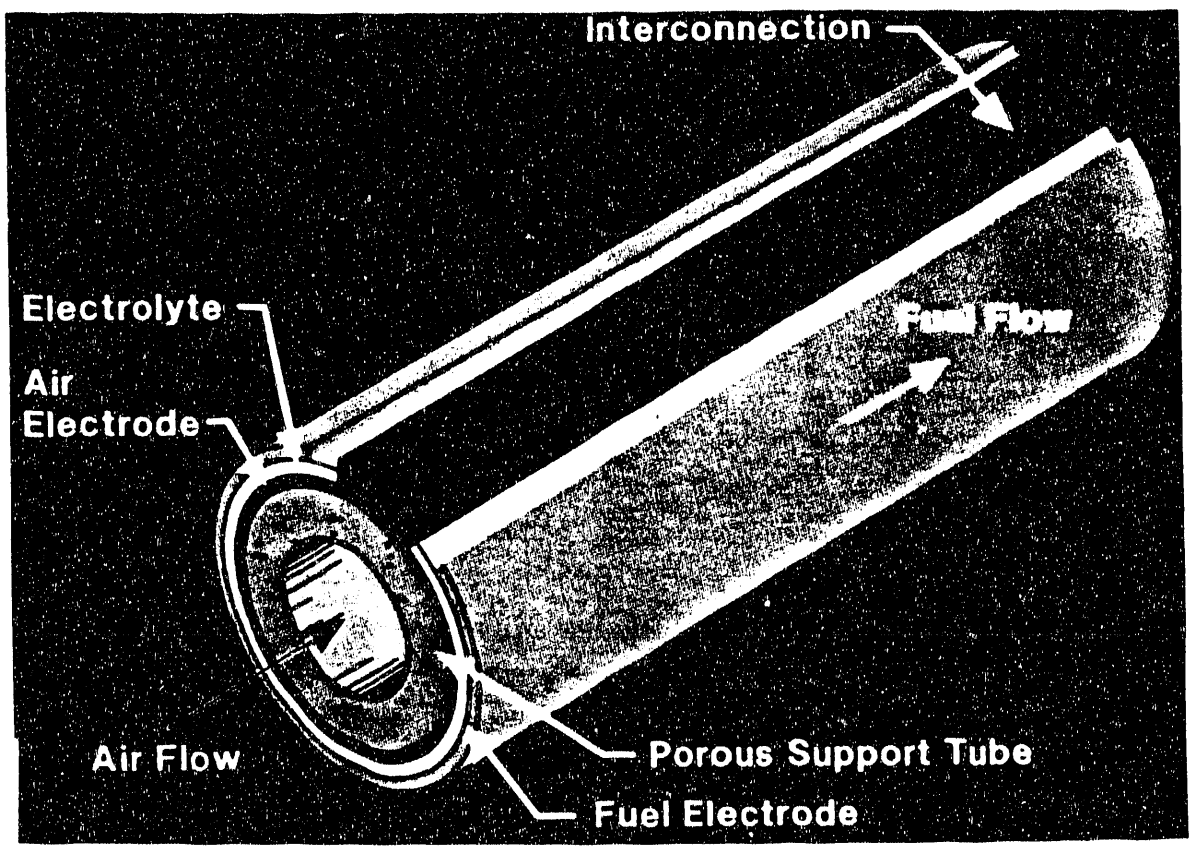

Figure 2.1 — Design of a porous tube supported solid oxide fuel cell.

plasma spray equipment offers the capability of high coating-feedstock (powder) throughput (3 kg hr^{-1}) and special high-power guns can achieve a feed stock throughput of over 25 kg hr^{-1}.

Plasma arc spray deposition[1] is a process in which the desired coating material in powder form is heated to near or above its melting point while being accelerated by a carrier gas stream through a high power electric arc. The powder is directed at the substrate (the surface to be coated), and on impact, forms a coating consisting of many layers of overlapping, thin, lenticular particles or splats.

The basic design of a plasma gun shown schematically in Figure 2.2 consists of two electrodes: a cone-shaped cathode (identified as electrode in Figure 2.2) inside of a cylindrical anode which extends beyond the cathode to form a nozzle. An inert gas -- usually argon with an admixture of hydrogen -- flows through the space between the electrodes, where it is ionized to form a plasma. A tube directs powdered coating material into the jet of plasma that develops in the nozzle. Water is circulated through passages in the anode and cathode to prevent melting of the electrodes.

The electric power applied to the gun, 30 to 40 kilowatts, results in a thermal plasma with a high enthalpy, or heat content. The temperature can approach 15,000°C.[2] The plasma also contains enthalpy associated with the ionization of gas atoms and dissociation of molecules. A plasma of hydrogen, a diatomic gas, has higher enthalpy at a given temperature than the plasma of monatomic argon. Hydrogen as a secondary gas added to the primary argon gas increases the ability of the gas to melt refractory oxides.

The internal geometry of the gun produces thermal and magnetic pinch effects that increase the pressure, temperature and velocity of the plasma. Depending on the gun geometry, gun power and gas flow, the plasma plume may reach supersonic velocities.

The powdered coating material is carried in an argon stream and is injected into the plasma either within the nozzle, or as the plasma exits the face of the anode (as shown in Figure 2.2). Effectiveness of a given plasma in melting and accelerating the powder depends on the type

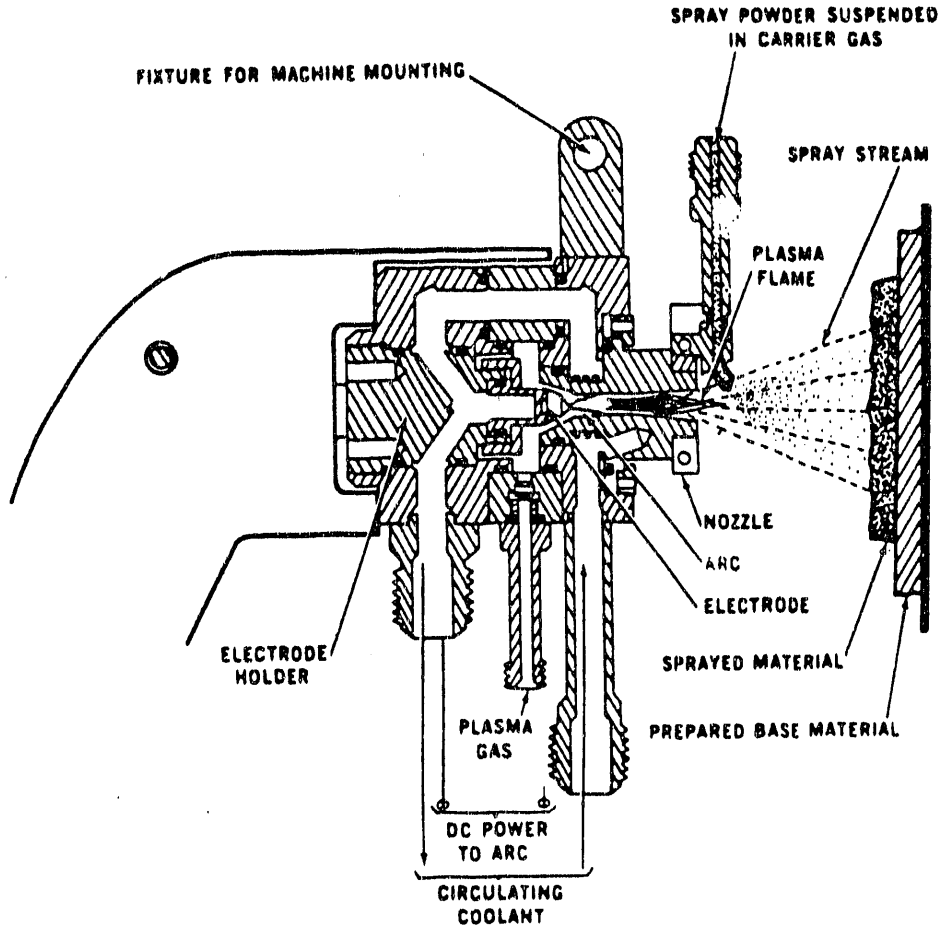

Figure 2.2 — Schematic of a plasma gun [after Ingham and Shepard (1965) as reported by Safai and Herman[1]].

of material and size and shape of the particles. For a given coating material and gun geometry there is an optimum particle size. Particles smaller than the optimum will overheat and volatilize; larger particles will not completely melt.

When particles are sprayed in air, the particles begin to cool and slow down as they collide with air molecules after leaving the plasma plume. An important factor in the coating process is the gun to surface distance, which is typically 5 to 10 cm for spraying in air.

The fast moving droplets of coating material solidify into "splats" on the target surface and accumulate into a coating at a rate that depends on the area to be covered, the powder feed rate and how rapidly the plume moves across the surface. Successive splats interlock mechanically and in ceramic coatings, sintering can consolidate the deposit.

Ceramic coatings in particular may contain cooling cracks and pores due to the entrapment of air in the deposit. The porosity increases the thermal insulating characteristics of the ceramic and the pores interrupt the propagation of cracks when the deposit is strained. Thermal barrier-type coatings where thermal insulation is required benefit from these structures.

However, in order to obtain gas-tight coatings, pores in the coating can be avoided by spraying in a chamber where gas is excluded (actually a low pressure atmosphere of the plasma gas). In such "vacuum" plasma spraying, no air is trapped and the droplets which are not decelerated by air resistance deposit at higher velocities compared to that in air so that the splats are spread flatter and thinner. However, in vacuum there is greater thermal coupling of the plume with the substrate increasing the possibility of thermal shock damage to ceramic substrates.

The plasma spray process, in general, is well suited for the processing of ceramic materials in the form of powdered feedstock. Oxide powders for plasma spraying are generally prepared in one stage or in a combination of stages of sintering, fusing or spray drying. In this program, spray dried powders were used. In spray drying, small constituent particles

are adhered by a binder, generally organic, which burns off in the plasma during the spraying.

The use of plasma arc spray deposition technology to solid oxide fuel cells was mentioned as early as 1970 by Rohr.[3] The electrodes sprayed, however, were deliberately porous. Nagata, Ohno, and Sato[4] fabricated a fuel cell stack using plasma and flame spraying techniques. They applied the electrolyte - yttria-stabilized zirconia - as a nearly gas tight film by plasma spraying. Both the anode and cathode applied by acetylene-oxygen flame spraying were deliberately porous.

Subsequently, Nagata et al.[5] reported on an improved stack of 12 cells connected in series by interconnectors. Their design consisted of a number of gas tight layers, such as alumina, electrolyte (yttria-stabilized zirconia) and interconnector (NiAl plus calcia-stabilized zirconia) made by dc plasma arc spray deposition. They found that the plasma spray method could make cell stacks in a short time and is suitable for automated manufacture. However, they acknowledged a need to improve the gas tightness of the seals.

Perovskite coatings of the composition $La_{0.8}Sr_{0.2}Co_{0.8}Ni_{0.2}O_3$ were plasma sprayed on nickel substrates by Murphy and King.[6] The plasma spraying had good coverage and adhesion, however, in their spraying the particles were softened but not completely melted in the plasma gas as high density of the coating was not required. Dense layers of yttria stabilized zirconia for a solid oxide fuel cell electrolyte were made by Ohno, Kaga and Nagata[7] with use of a dc arc plasma spray technique. They reported fabricating a 200 μm thick layer with 96.6% density, apparently sufficiently dense as not to pass gas. The thick electrolyte was a significant portion of the cell internal resistance. Aware that a thinner electrolyte would increase the output power of the cell they indicated doing laser beam treatment of electrolytes less than 100 μm in thickness to obtain higher density. They found that 50 μm was the minimum thickness of coating due to the formation of cracks and pinholes.

A new design of plasma gun described by Itoh, et al.[8] produced yttria-stabilized zirconia coatings that were denser than coatings produced

by conventional plasma guns. Their gun has the plasma gases fed separately from the inert gases that protect the cathode and anode, making it possible to use oxygen or air as a plasma gas. Other attributes of the gun are a stable high temperature plasma plume, ability to inject the powder into the region of highest temperature and maintain stable powder feed rates for a long time. At any differential pressure of hydrogen, at 25°C, coatings sprayed with the gun had only 45% of the gas permeability of coatings sprayed with conventional guns.

A problem in the plasma arc spraying of doped lanthanum chromite powder is the volatility of the material, discussed by Meadowcroft[9]. Pure and doped lanthanum chromites have appreciable volatility. The volatility is preferentially of chromic oxide, but even from pure lanthanum chromite it is proportionately much less than from pure Cr_2O_3. In the case of Cr_2O_3 the evaporation is known to be caused by loss of CrO_3 gas and this process presumably occurs in $LaCrO_3$ also.

While there are many variables that influence the plasma-arc spraying process, about twelve have been identified as having the most influence on coating properties. Improved control of these variables has been the focus of improvements in the spray equipment manufacturing industry. These include incorporating empirical or real-time feedback looping, redesigning fundamental gun components and feedstock powders and innovative power-supply design.

3. Fabrication of Gas-Tight Interconnection Layer

The principal task in this program was to fabricate a gas-tight layer of interconnect on tubular air electrode substrate with atmospheric plasma arc spray deposition. The main requirements of the layer were that it be thin (40 to 60 μm thick), of uniform thickness along the length, of suitably doped $LaCrO_3$ and demonstrate a vacuum leak rate in air of less than 1.0 mm Hg min^{-1} for a strip 9 mm wide by approximately 15 cm long.

Other tasks included measurement of the physical and chemical properties of the interconnect strip, electrical properties of the strip and associated air electrode substrate, and fuel cell fabrication, qualification and performance testing.

Optimization of the spray parameters depended initially on a simple physical, electrical and microstructural evaluation of the sprayed layer. The evidence of structural cracks, voids, multiple phases, thickness variations, etc. after each spray trial provided information as to which variables needed to be adjusted to alleviate the problem. The key qualifiers for the optimization of the spray parameters were microstructure and chemistry.

Gas tightness was estimated initially using a liquid penetration test. The physical and chemical microstructure was determined by use of vacuum impregnation with resin epoxy and then metallographic sectioning. Depending on the microstructure, the chemistry of the coating was determined using the scanning electron microscope with energy dispersive analysis of X-rays or electron beam techniques. Deposit thickness and bond quality were estimated from the metallographic sections.

Electrical conductivity tests initially were done at room temperature with use of a low impedance volt-ohmmeter. The measurements were made across a one centimeter spacing of graphite spots for the probes to minimize contact resistance. In practice, electrical conductivity measurements showed low values (hundreds of ohms) for coatings of a wide range of chemistries, densities and thicknesses, and thus, were of limited usefulness in the characterizations of coatings.

3.1 PLASMA SPRAYING

3.1.1 Equipment Description

Several plasma spray systems were utilized in spraying the interconnect layer. They all were capable of spraying the coating as they allowed the use of optimum spray parameters.

A lightweight, 40 kW general purpose hand-held gun and a 55 kW machine-mounted gun were used with two different plasma spray control units. A unit with flow meter tubes and needle gauges was used only with the hand-held gun. The other unit -- a microprocessor-based plasma controller with mass flow meters and complete digital displays for the parameters -- was used with both guns.

The powder feeders were either volumetric or fluidized bed-types. The volumetric feeder with a built-in powder stirrer was found to be more effective in feeding the spray dried powders.

Since the traverse velocity of the microprocessor-based plasma controller was not high enough to minimize heat build-up in the substrate, a special high velocity linear track was built. This unit had a slide track onto which the hand held gun was mounted and moved along the x-axis. Using this unit, the spray distance and traverse speed could be better controlled for the application of sprayed deposits to longer tubular substrates than with the hand held gun. The tube could be rotated in order to maintain the perpendicularity of the plume to the cylindrical substrate.

Another special apparatus used in the investigation was a furnace which allowed spraying the tubular cells while being heated.

3.1.2 Spray Parameter Test Matrices

In the design of a spray matrix, the principal spray variables such as gun power, primary and secondary plasma gas flows, powder feed rates, gun to substrate spray distance and substrate temperature are varied to find the parameters that along with powder of the requisite chemistry and particle size distribution produce a gas tight coating. Each principal spray variable discussed below in detail has an effect on the deposit characteristics that can be described only in general terms as there are no truly independent variables. When the value of a single spray variable is changed, the influence on the deposit quality depends on the magnitude of the other variables. Each principal variable is described only in terms of the ranges and components actually used in this program.

Plasma Gun or Torch -- even the same gun does not usually spray reproducibly unless serviced periodically to eliminate degradation due to erosion and fouling. Guns of different designs and bores are not expected to spray with comparable results unless many of the other variables are adjusted accordingly. Therefore, the present program restricted the investigation to two gun designs with concentration on the lightweight 40 kW general purpose gun. For most of the test matrices, the gun type was not a variable.

Plasma Power -- also known as gun power, is an important variable in controlling the melting of the powder particles. The current used was generally 450 to 650 amperes, but the secondary gas flow, especially with hydrogen, controlled the voltage of the plasma. Higher current levels would heat powder particles to higher temperatures and cause more volatilization of some constituent oxides.

Plasma Gases -- the primary gas used was argon with additions of 5 to 25 volume percent secondary gases such as hydrogen or helium. Hydrogen had a strong effect on the velocity, heat content and, the overall

power of the plasma gas. Helium, as a secondary gas, by comparison imparted less heat content and velocity to the plasma gas. Therefore, the control of the heat content and temperature of the plasma gas for a particular gun type with a specific nozzle was regulated by the choice of arc current, types of secondary gases, and ratios of primary to secondary gases. Higher volume percentages of hydrogen in the secondary gases could cause more volatilization of some constituent oxides from the powder particles. Also there would be more localized heating of the substrate at a given spray distance.

Carrier Gas Flow – argon was used to inject the powder particles into the plasma gas. This variable was adjusted relative to the plasma gas parameters to achieve particle penetration into the plume. Insufficient gas flow may prevent some powder particles from penetrating the plume and thus becoming molten.

Powder Injection – injections of particles counter to the plasma gas flow direction facilitates heating of the particles by increasing the dwell time of particles within the core of the plume. Injection downstream, conversely does not heat the particles as much as counter injection. Variable port diameters and injection angles were briefly investigated with the same bore diameter. For most of the test matrices a perpendicular powder particle injection into the plasma plume at a fixed distance from the nozzle was used.

Powder Feed Rate – this variable was investigated considerably because of its effect on the deposit deposition rate and quality of deposit microstructure. High feed rates relative to the heat content of the plasma plume can result in imprecise melting of the powder particles resulting in pockets of porous coating.

Spray Distance – in this investigation 7 to 13 cm was used. The molten powder particles should be at an optimum temperature and velocity depending on the values of the other variables such as secondary gas type and gun current.

Gun Traverse Velocity – due to the thermal shock sensitivity of the substrate, it was important to minimize heat buildup in the substrate by rapid movement of the plume relative to the substrate surface. The

number of passes were increased to compensate for the low deposition rates obtained at rapid movement of the plume.

Substrate Temperature -- the magnitude of this variable does have an effect on the deposit quality. The closer the substrate temperature is to the freezing temperature of the deposit, the lower the residual stresses will be in the coating when the deposit cools. This will be particularly true if the substrate and coating materials have similar coefficients of thermal expansion. The magnitude of macro- and microcracking is influenced by the level of stress and strain developed when the sprayed oxide cools. A high substrate temperature promotes splat sintering and interdiffusion to reduce chemical inhomogeneities. In addition, a high substrate temperature diminishes thermal shock by promoting stress relaxation by creep deformation.

Powder -- the spray dried powders consist of nearly spherical aggregates of small particles. The coarser sieve fractions for example -270, +325 mesh (-53 μm, +45 μm) were reasonably free of fines, that is -10 μm. The greater the -10 μm fraction the greater was the difficulty in feeding the powder at a uniform rate. Also, the finer particles if injected into the plume undergo more differential volatilization than the larger particles. Since the smaller particles are decelerated more readily in air and lose heat rapidly by radiation they may solidify before depositing.

Some trials were done with the coarser particle distributions (-270, +325 mesh); however, most of the spray matrices used a finer particle size distribution.

3.2 RESULTS OF SPRAY TRIALS

Spray-dried Sr-doped $LaCrO_3$ powders were characterized with the scanning electron microscope-energy dispersive system (SEM-EDS) for powder morphology and chemical homogeneity. Figure 3.1 shows the -270, +325 size fraction (<53 μm and >44 μm) to consist principally of aggregates of micron-sized particles. The aggregates are either solid or hollow. This is typical for these types of spray-dried powders. The

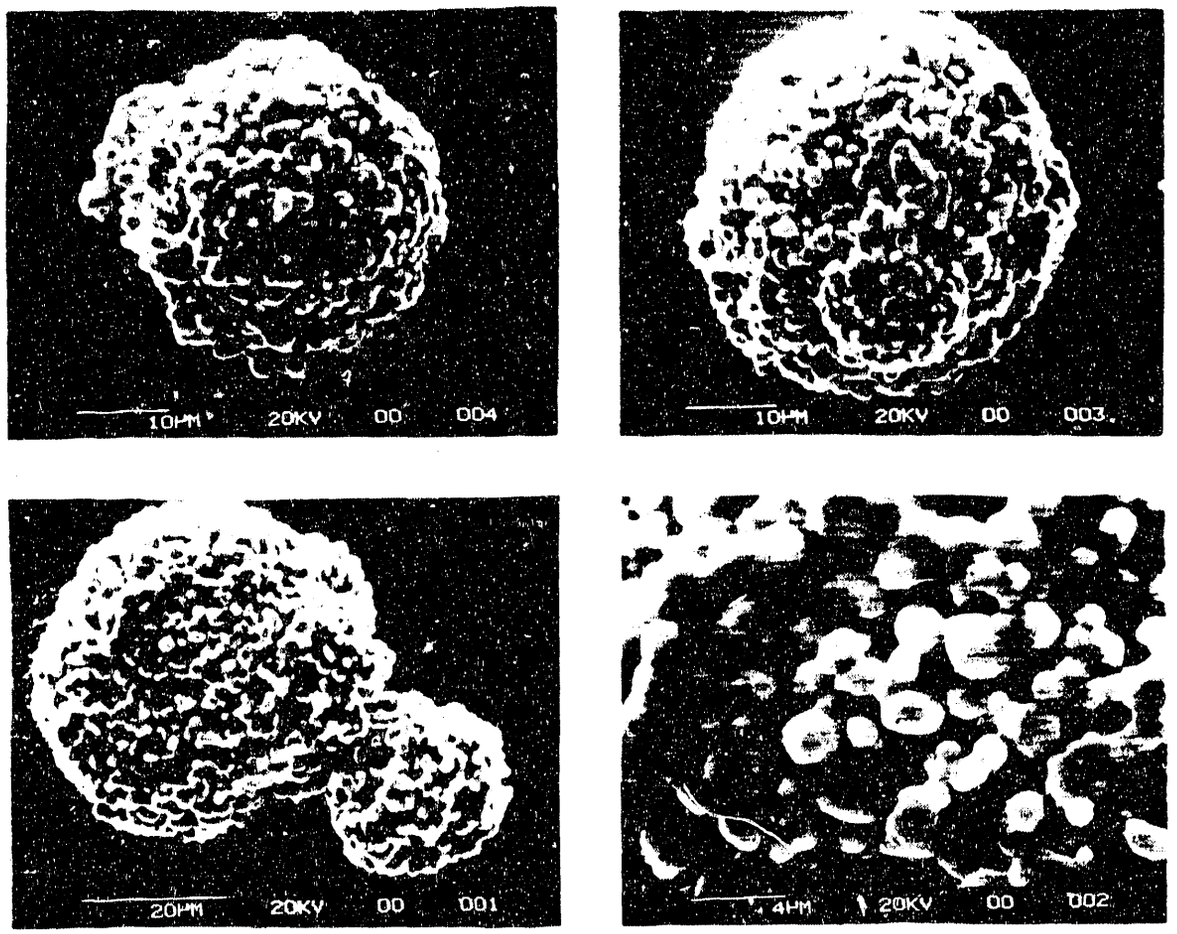

Detail of large particle at left

Figure 3.1 — Spray dried Sr-doped $LaCrO_3$ powder.
-270 mesh +325 mesh size fraction

finer mesh size fraction consists essentially of smaller agglomerated particles but may contain fragments of the larger agglomerated particles. Electron beam microanalyses of the powders showed the agglomerated particles to be chemically homogeneous.

Preliminary spray trials were made on 10 cm lengths of sintered air electrode supported on a porous calcia-stabilized zirconia tube. The air electrode substrates had been wet sanded to produce a uniform surface finish. A metal mask with a 9 mm vertical opening was used to produce a sharp coating edge without edge buildup. These spray trials were conducted to identify variables with the greatest influence on the quality of the coating. The matrix of experiments varied gun power, spray distance, and powder feed rate. The deposition rates for individual parameter sets varied and the number of passes of the gun were adjusted to obtain a coating thickness of 130 to 230 μm. Thick coatings were sprayed for convenience of evaluation. Gun amperage and primary and secondary plasma gas flows had the largest effect on the coating structure. Also, the lower the deposition rate of the coating per pass, the better was the splat structure. Figure 3.2 shows photomicrographs obtained with use of the scanning electron microscope (SEM) of structures formed with different plasma gas chemistries. Trial 1 was made at a lower Ar/H_2 ratio than Trial 2. The effect of a lower Ar/H_2 ratio was to produce a more consolidated deposit but there was also more chemical inhomogeneity. Figure 3.3 shows the effect of increasing the gun power with a fixed Ar/H_2 plasma gas ratio. This trial, No. 9, gave a denser coating than Trial No. 1 (both were at the same Ar/H_2 plasma gas ratio) but showed more chemical inhomogeneity. The micrographs made with secondary electron emission generally show mostly surface relief features; the micrographs made with backscattered electrons can show differences in chemical composition based on atomic number differences. The lighter tone phases have a higher average atomic number than the darker tone phases. In the case of the Sr-doped $LaCrO_3$ composition the La-richer phases have lighter tones; the basic powder composition has the darker tones. Figure 3.3 also shows the uniformity of coating coverage on the inherently porous air electrode

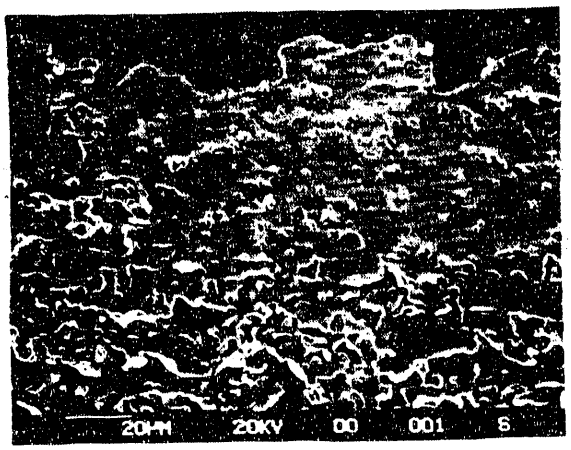

Trial 1 - Secondary electrons

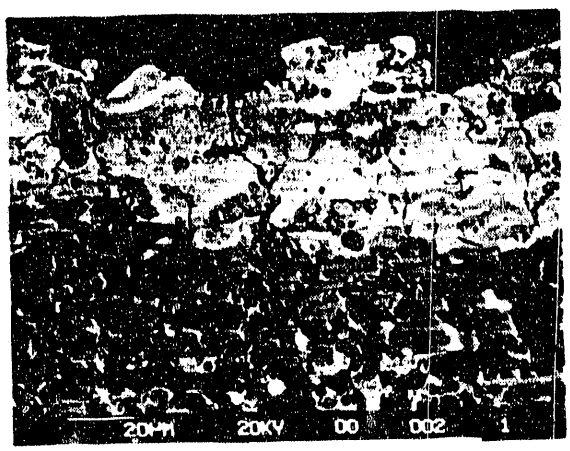

Trial 1 - Backscattered electrons

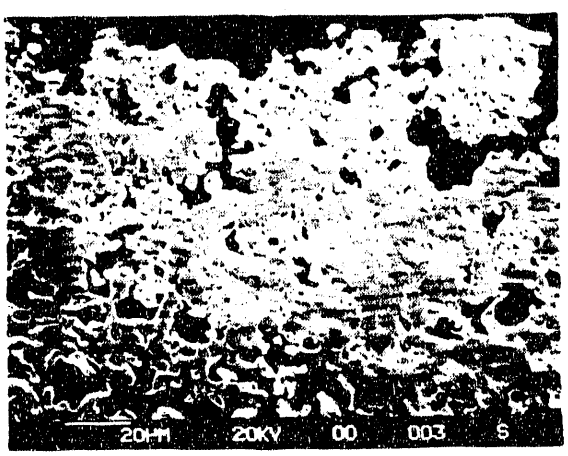

Trial 2 - Secondary electrons

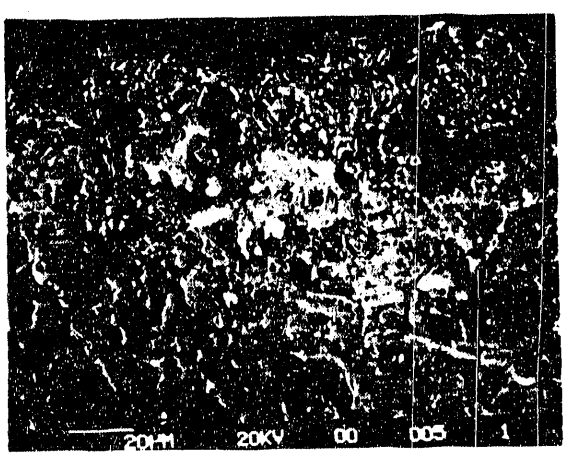

Trial 2 - Backscattered electrons

Figure 3.2 — Plasma-arc sprayed Sr-doped $LaCrO_3$. -270 mesh powder. Substrate grit blasted prior to spraying.

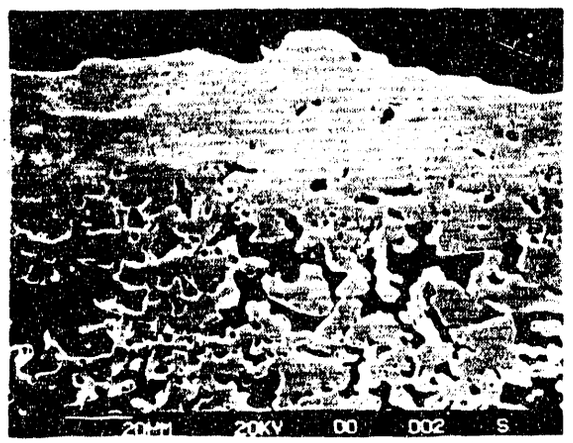

Right of center - Secondary electrons

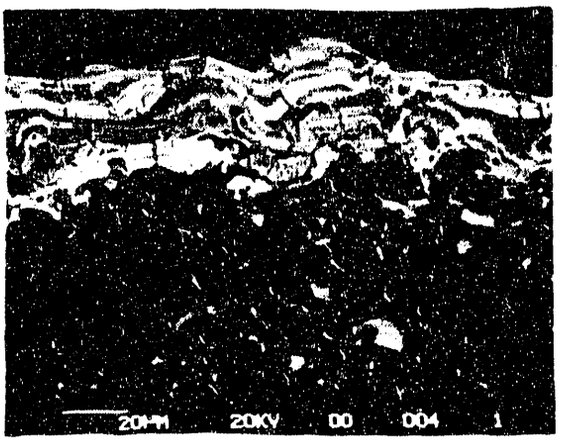

Right of center - Backscattered electrons

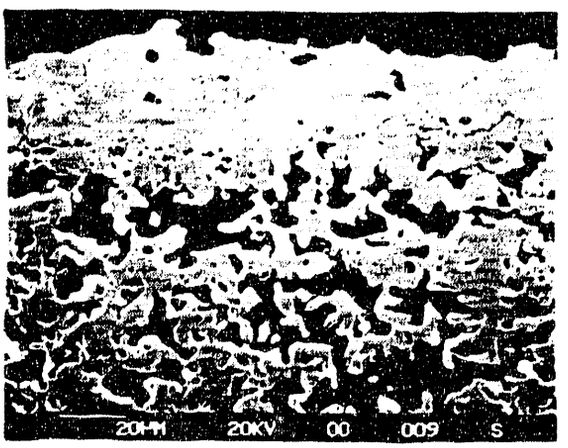

Center of layer - Secondary electrons

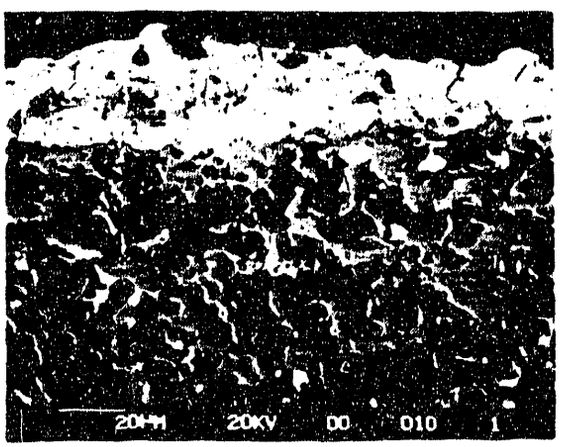

Center of layer - Backscattered electrons

Figure 3.3 — Plasma-arc sprayed Sr-doped $LaCrO_3$ at higher gun power.
-270 mesh powder. Substrate sanded prior to plasma spraying.

substrate. Figures 3.2 and 3.3 show that the deposit is fairly well bonded to the substrate over a range of gun power and plasma gas chemistry settings.

Trials 1 and 9 were also with substrates of widely differing surface finishes. The substrate of Trial 1 (as well as Trial 2) had been grit blasted to roughen the surface. The substrate surface of Trial 9 had been wet sanded with 600 grit paper. In both cases, there was good deposit adherence. The smoother substrate, however, produced a deposit of more even thickness compared to the grit blasted substrate.

The coatings had, in addition to porosity and chemical inhomogeneity, small cracks aligned principally normal to the plane of the deposit. The cracks were more prevalent in the deposits formed at the higher power and/or lower Ar/H_2 plasma gas ratios. The cracks probably resulted from the combination of chemical inhomogeneity and temperature gradient across the coating to the substrate.

Subsequent spray trials established the values of the spray variables found influential in producing through-defect free coatings. These variables were:

- number of gun passes (increased number reduces through-defects)
- gas flows (primary and secondary)
- gun power
- location of entry point of powder port relative to the nozzle surface and center line of the nozzle opening.

The traverse speed with each parameter set was varied to produce a coating between 50 and 100 μm in thickness. Coating evaluation, as anticipated, indicated that the lower the deposition rate per pass, the lower the density of interconnected pores. Each layer had some defects (pores, pockets of chilled particles) but increasing the number of layers while maintaining a final total thickness by decreasing the amount deposited during each pass, decreased the probability that defects would be interconnected through the thickness of the coating.

The quality of each thin successive coating was influenced by the surface roughness of the substrate. Many defects in the coating were

related to the larger pores in the substrate surface. Very large surface pores (up to 175 μm in diameter) could not be either bridged or the pore surface coated in a continuous manner. Some surface roughness was required for mechanical adherence of the coating but, ultimately, substrate roughness limited the quality of the coating.

Spray trials were made with use of two different gun and spray systems in an effort to solve the problem of differential volatilization losses from the sprayed particles. The Sr doped $LaCrO_3$ powder was sprayed at different gun currents both under air plasma spray (APS) and vacuum plasma spray (VPS) conditions. The VPS system used a low pressure of an inert gas. Figure 3.4 shows backscattered electron micrographs of polished cross sections of some of the sprayed coatings. All the coatings had porosity and some cracking. The lighter toned areas in the micrographs in Figure 3.4 are La-richer splats.

Heating the substrate prior to spraying and holding the temperature during spraying to reduce the incidence of cracking within the coating was also attempted. An illustration of this effect is shown in Figure 3.5 where the substrate was heated sprayed and then slow cooled. The coating was dense enough to resist penetration by both water and acetone. The coating, however, still showed chemical inhomogeneity, as evidenced by the lighter tones of some of the splats in the backscattered electron micrograph. The lighter tone splats correspond to the lanthanum rich phase.

The coatings sprayed on the preheated substrate were very dense except for some internal shrinkage cracks. The lanthanum-rich phase had more shrinkage cracks than the Sr-doped $LaCrO_3$-base phase which suggests that the former phase has a somewhat different coefficient of thermal expansion. The coatings were well bonded and probably would have been gas tight if the internal shrinkage cracks could have been avoided.

Optimum values of the spraying variables were used to deposit interconnect strips on full length air electrode over porous support tubes. The substrate had been heated and sprayed with while in the slotted cylindrical furnace. Figure 3.6 shows the as-sprayed microstructure at

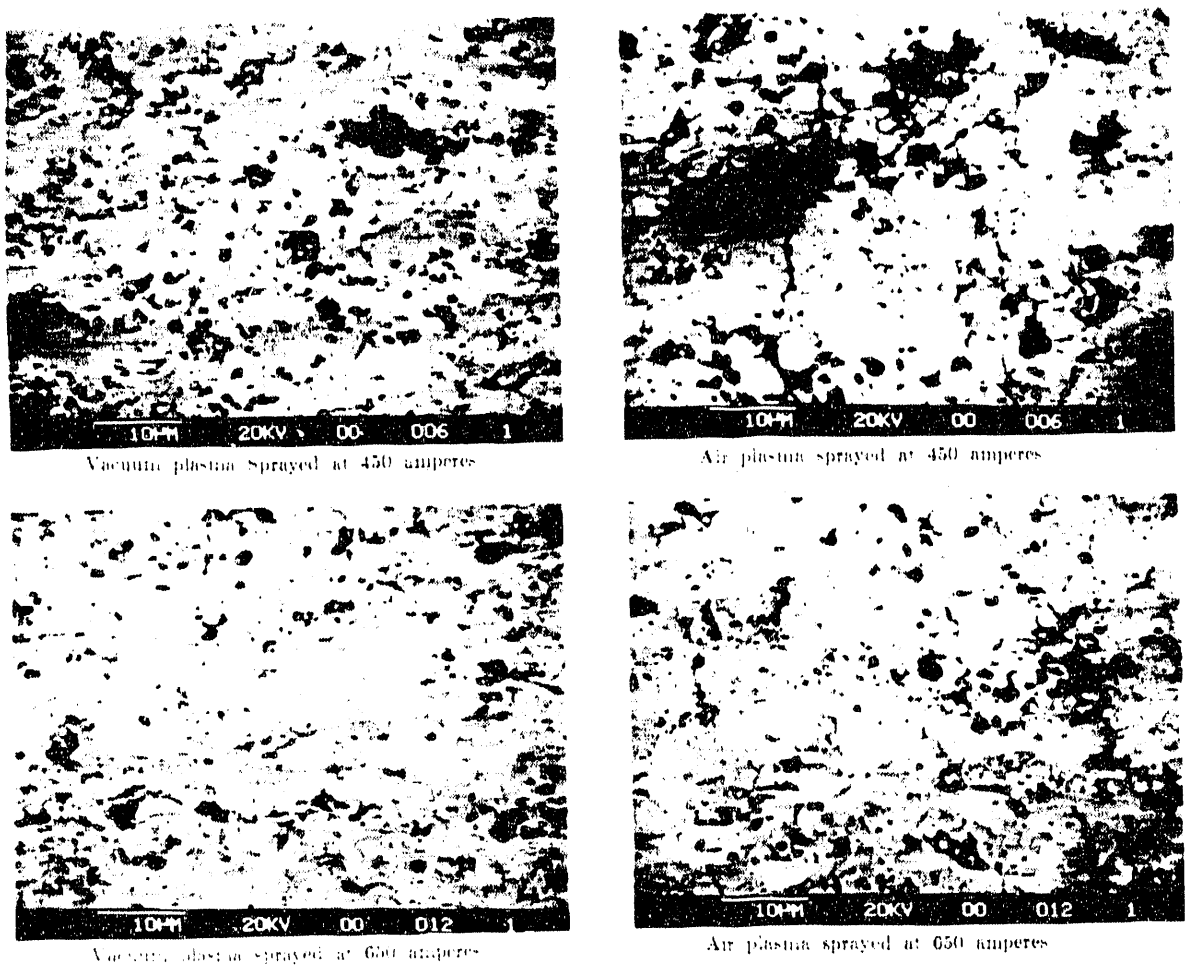

Figure 3.4 — Backscattered scanning electron micrographs of polished cross sections of plasma arc sprayed Sr-doped $LaCrO_3$.

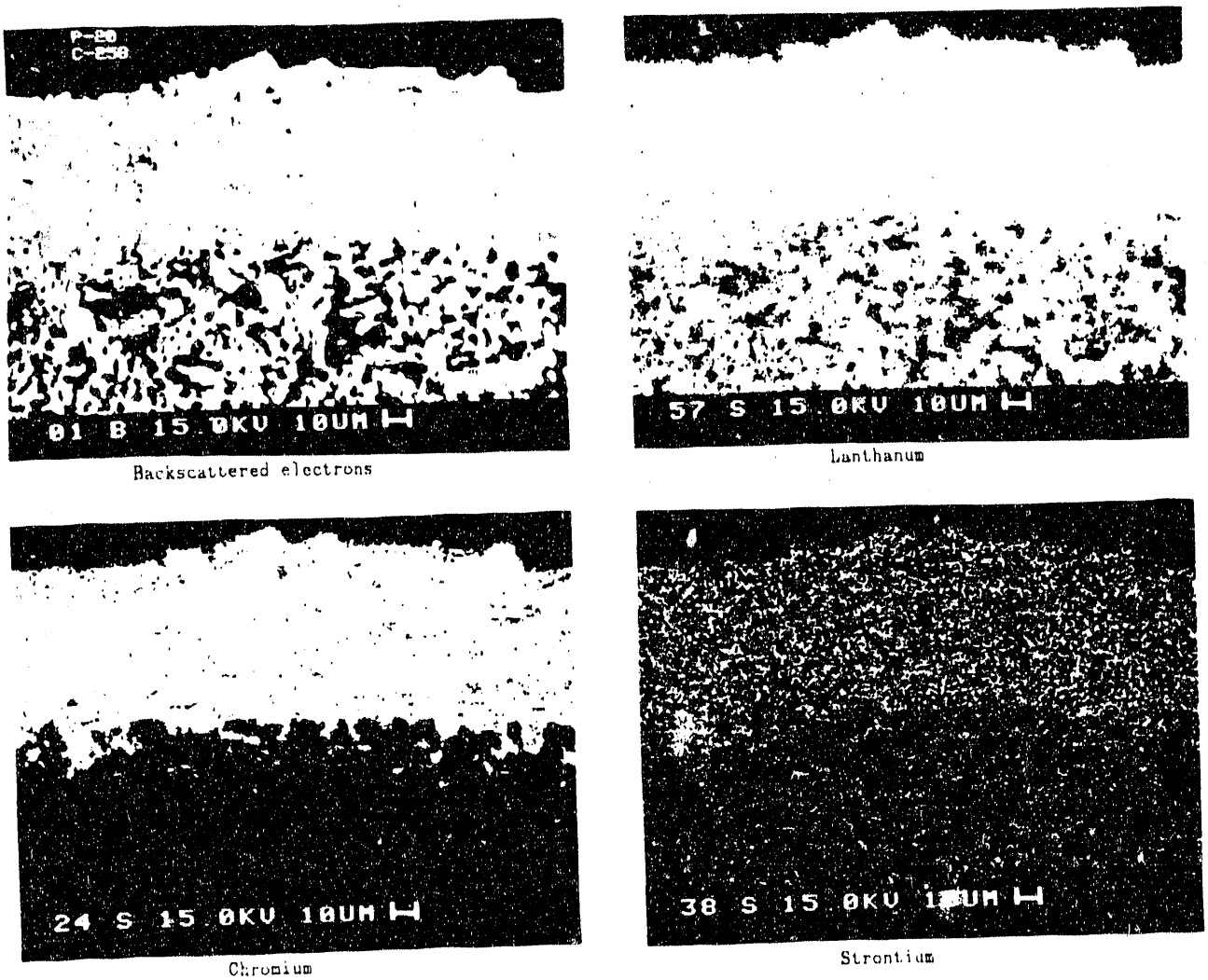

Figure 3.5 — Elemental maps of coating sprayed at low gun current. Sprayed on preheated substrate.

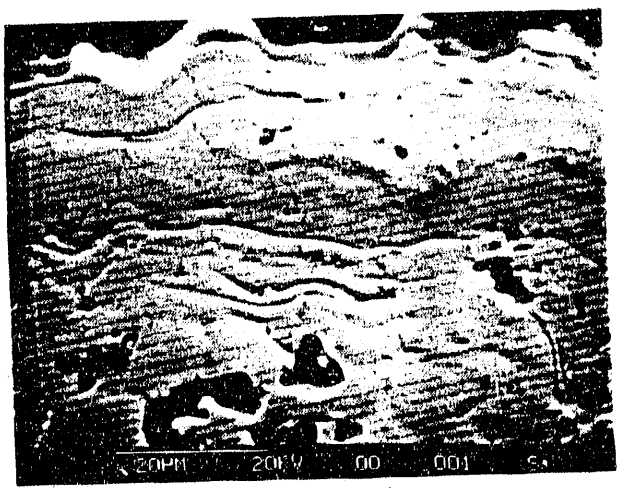

Area 1 - Secondary electrons

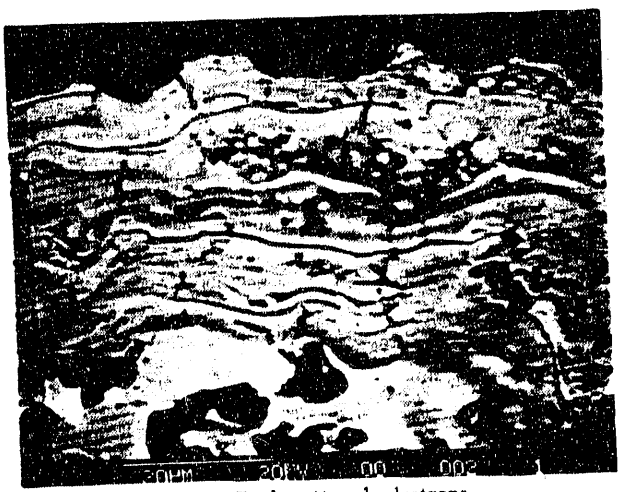

Area 1 - Backscattered electrons

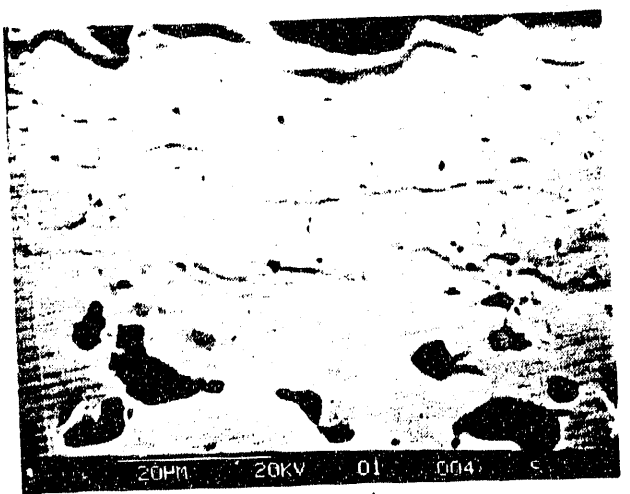

Area 2 - Secondary electrons

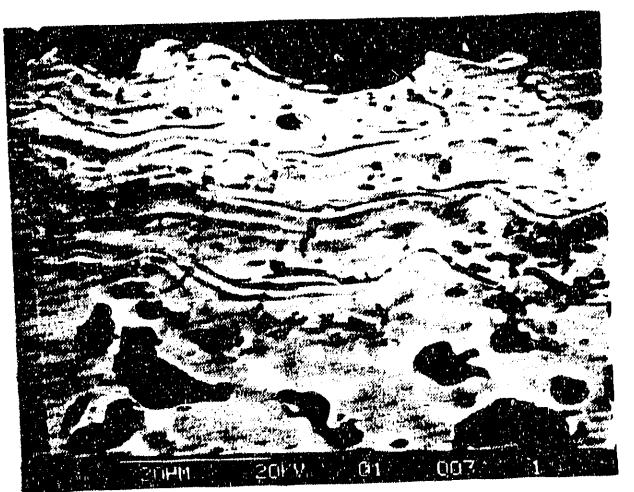

Area 2 - Backscattered electrons

Figure 3.6 — As-sprayed microstructure at two different locations along the length of the tube. Deposit was sprayed on heated substance.

two different locations along the length of the tube. The sections had been polished with a fine abrasive to accentuate the hardness differences in the deposit. There was good bonding of the deposit to the substrate.

Six thin wall supported tubular cells were sprayed with interconnect using the best combination of spray variables including heated substrates. Difficulty was encountered subsequently in sealing the borders of the sprayed interconnect adequately to measure the gas tightness of the layers. The borders of the plasma-sprayed interconnects were sufficiently rough and uneven to prevent sealing in the processing of the tubes to make complete cells. Helium leak checks indicated that the preponderance of leaks were along the border seals, with only a few actually within the deposit. The interconnect surfaces were rough, free of hairline cracks, and had some deep pits where material had pulled out in the post-spraying cleaning process.

Four of the above cells were processed for the deposition of a fuel electrode. Figure 3.7 shows the interconnect strips of the completed cells before the application of nickel plate to the interconnects. The white streaks at the edges and within the 15 cm by 7 mm boundaries of the interconnect are adherent layers of zirconia which deposited under the masking. The masking cracked and lifted in a few places during the application of the fuel electrode. The zirconia was left in place in order to prevent damage to the plasma-sprayed interconnect strip.

After the application of nickel plate on the interconnect strips the cell leak rates were low enough to allow electrical testing of at least one cell.

Figure 3.8 illustrates the electrical performance of one cell. The voltage at a current density of 350 mA cm^{-2} was comparable to that of a cell with an interconnect made by the present electrochemical vapor deposition (EVD) process. The cell resistance index was also comparable.

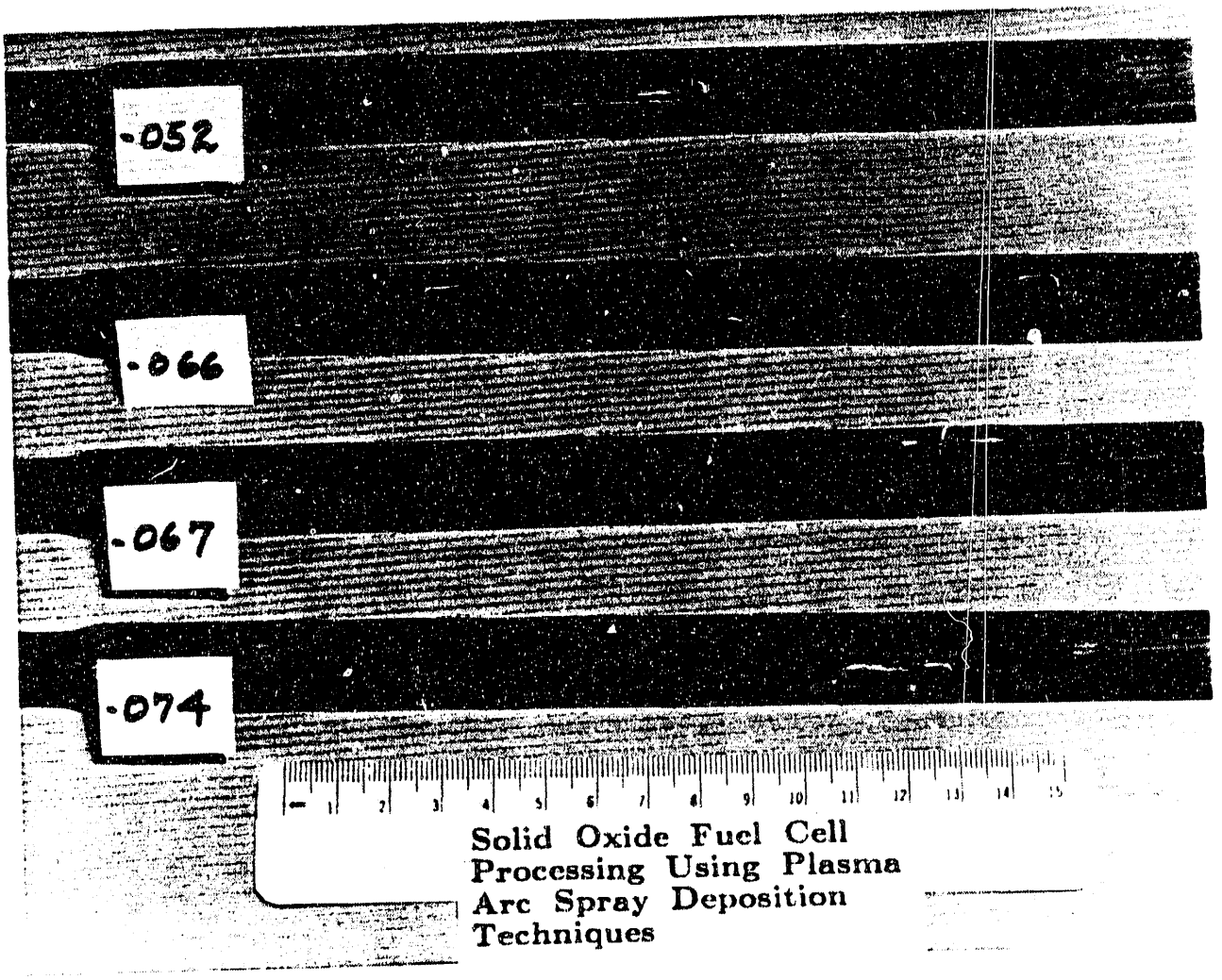

Figure 3.7 — Four fully processed cells (except for nickel plating). Interconnect strips are 15 cm x 7 mm. White streaks are zirconia deposits that formed through thin areas in the masking during cell processing. (Numbers shown at the left end of the cells are cell test numbers.)

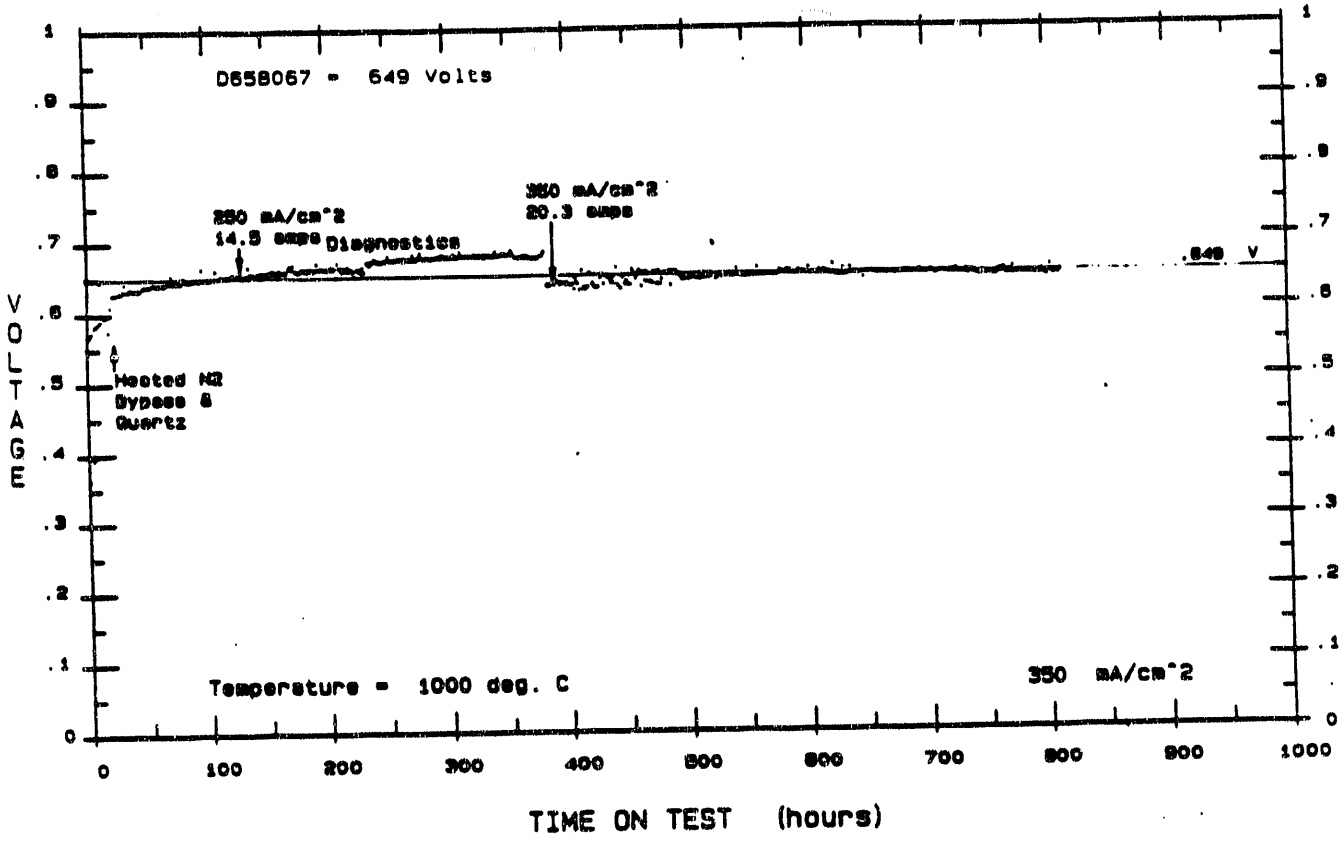

Figure 3.8 — Electrical performance of a cell with a plasma-sprayed interconnect strip.

4. Discussion, Conclusions, and Recommendations

The use of a basically Sr-doped $LaCrO_3$ spray dried powder, rapid gun traversing, a microprocessor-based plasma spray control unit and a lightweight 40 kilowatt plasma gun produced a dense interconnect layer; however, there were still slight chemical inhomogeneities and some microcracking in the as-sprayed layer.

The program utilized exclusively sprayed dried oxide powders which were somewhat fragile nearly spherical aggregates of the constituent oxides. In spite of careful sieving there was a tendency for the powder fraction collected for spraying to contain several percent of fines. During the subsequent spraying process the fines suffered greater volatilization than the coarser aggregates. Spraying at atmospheric pressure in air probably resulted in the increased La/Cr ratio of the droplets. Spraying under conditions of a low pressure of inert gas in the absence of oxygen also increased the La/Cr ratios of the droplets.

The microcracking found in the sprayed deposits was somewhat exacerbated by chemical inhomogeneity but also persisted in coatings almost compositionally correct. The microcracking was a consequence of the inability of the sprayed lanthanum chromite to creep sufficiently to alleviate tensile stresses as it cooled from the molten state to the temperature of the substrate. Expanding the substrate by suitable preheating and giving the substrate/deposit system (the $LaSrCrO_3$ based interconnect and the $LaSrMnO_3$ based air electrode substrate have closely matched thermal expansion coefficients) a slow cool to room temperature can avoid macrocracking; however, there was some persistence of microcracking. At the higher preheated substrate temperatures the resulting microcracks were

fewer and less interconnected. The substrate, however, would have to be heated close to the solidification temperature of the droplets to prevent microcracking. As the droplets are probably in excess of 2500°C when they strike the deposit, it is not practical to heat the substrate to this temperature. The use of a graded density bond layer of lanthanum chromite between the substrate and the dense sprayed coating also did not reduce the degree of formation of microcracks. Prevention of microcracking was not achieved and this is an area where continued investigation is essential.

A dense, adherent, compositionally acceptable coating was produced but it turned out to be difficult experimentally to produce a completely gas tight deposit. The microstructure of the sprayed deposit made it difficult to effect a gas tight seal around the deposit in order to isolate the remainder of the porous air electrode from the sprayed interconnect strip. The rough sprayed surface was ground and sanded but it could not be leveled sufficiently to make gas tight seals in the subsequent cell processing steps. Hence, the gas tightness of the sprayed strips could not be determined accurately. The sprayed strips had pin point leak sites, some of which were related to damage incurred by cleaning. It is recommended that future work be devoted to achieving reliable seals between the sprayed lanthanum chromite and other materials used in solid oxide fuel cell such as yttria-stabilized zirconia.

The successful testing of a cell with a plasma-arc sprayed interconnect demonstrated that the sprayed interconnect can withstand the cell processing steps and has the potential to perform electrically comparable to an electrochemically vapor deposited interconnect.

The quality of the plasma-arc sprayed strontium-doped lanthanum chromite is sufficient at this stage to recommend initiation of physical and chemical property measurements of the deposits, specifically, interconnection/substrate bond strength, thermal stability, residual stress, thermal expansion, RF inductive loss, and electrical conductivity. The spray process is optimized enough to provide reproducible and consistent test samples for the measurements.

The near success in forming a gas tight, compositionally adequate interconnect of a highly doped electronic conducting oxide suggests that further investigation can improve the process to the point of commercial feasibility. The use of the advanced spray-control systems can then be anticipated to effect a significant cost reduction in the production of solid oxide fuel cells.

6. Acknowledgements

The authors acknowledge invaluable contributions of the following individuals in the planning and execution of this investigation:

- Mr. G. Bancke for the skillful operation of the spray equipment and deposition of the coatings.

- Messrs. W. E. McMunn, T. M. Burke, and A. Pavillian for metallographic and microscopic examination of the coatings.

- Messrs. A. Karanovich and R. W. Palmquist for electron scanning and microprobe analyses.

In addition, we gratefully acknowledge the helpful discussions, especially in the preparation of the report, of the professional and management staff of the Advanced Energy Conversion Department. Lastly, appreciation is given to Mrs. J. A. Radford for her tireless efforts in the preparation of this report.

7. References

1. S. Safai and H. Herman, "Plasma-Spray Materials," *Treatise on Materials Science and Technology*, pp. 183-214, Academic Press, 1981.

2. H. Herman, "Plasma-Sprayed Coatings," Scientific American, pp. 112-117, September, 1988.

3. F. J. Rohr, "High Temperature Fuel and Electrolysis Cells with Zirconia Solid Electrolytes," *Applications of Solid Electrolytes*, pp. 196-205, JEC Press, Inc.: Cleveland, 1980.

4. S. Nagata, Y. Ohno, and H. Sata, "Development of High Temperature Solid Electrolyte Fuel Cells at Electrotechnical Laboratory," *Applications of Solid Electrolytes*, pp. 193-195, JEC Press, Inc.: Cleveland, 1980.

5. S. Nagata, et al., "Development of High Temperature Solid Oxide Electrolyte Fuel Cells," pp. 827-832, *IECEC*, Vol. II (1984).

6. G. J. Murphy and H. W. King, "Ceramic Electrocatalysts for the Oxygen Evolution Reaction-II: Plasma Sprayed Perovskite Coatings," Journal of the Canadian Ceramic Society, pp. 14-20, Vol. 54, 1985.

7. Y. Ohno, Y. Kaga, and S. Nagata, "A Study on the Fabrication and the Performance of the Solid Electrolyte Fuel Cell," Electrical Engineering in Japan, pp. 59-67, Vol. 107, No. 1, 1987.

8. T. Itoh, et al., "New Plasma Spraying System Without Tremendous Noises and Intense Rays," Proceedings of ATTAC '88 (The International Symposium on Advanced Thermal Spraying Technology and Allied Coatings), pp. 99-102, May 1988.

9. D. B. Meadowcroft, "Some Properties of Strontium-Doped Lanthanum Chromite," British Journal of Applied Physics (J. Phys. D), pp. 1225-1233, Ser. 2, Vol. 2, 1969.

10. H. Herman, "Advances in Thermal-Spray Technology," Advanced Materials and Processes, pp. 41-45, April, 1990.

END

DATE FILMED

10/9/92